Spheroid-based drug screen: considerations and practical approach

Juergen Friedrich[1,2], Claudia Seidel[1], Reinhard Ebner[3] & Leoni A Kunz-Schughart[1]

[1]OncoRay-Center for Radiation Research in Oncology, Tumor Pathophysiology, Faculty of Medicine Carl Gustav Carus, Dresden University of Technology, 01307 Dresden, Germany. [2]Institute of Pathology, University of Regensburg, Franz-Josef-Strauss-Allee 11, 93053 Regensburg, Germany. [3]Avalon Pharmaceuticals Inc., 20358 Seneca Meadows Parkway, Germantown, Maryland 20876, USA. Correspondence should be addressed to L.A.K-S. (leoni.kunz-schughart@oncoray.de).

Published online 12 February 2009; doi:10.1038/nprot.2008.226

Although used in academic research for several decades, 3D culture models have long been regarded expensive, cumbersome and unnecessary in drug development processes. Technical advances, coupled with recent observations showing that gene expression in 3D is much closer to clinical expression profiles than those seen in 2D, have renewed attention and generated hope in the feasibility of maturing organotypic 3D systems to therapy test platforms with greater power to predict clinical efficacies. Here we describe a standardized setup for reproducible, easy-handling culture, treatment and routine analysis of multicellular spheroids, the classical 3D culture system resembling many aspects of the pathophysiological situation in human tumor tissue. We discuss essential conceptual and practical considerations for an adequate establishment and use of spheroid-based drug screening platforms and also provide a list of human carcinoma cell lines, partly on the basis of the NCI-DTP 60-cell line screen, that produce treatable spheroids under identical culture conditions. In contrast to many other settings with which to achieve similar results, the protocol is particularly useful to be integrated into standardized large-scale drug test routines as it requires a minimum number of defined spheroids and a limited amount of drug. The estimated time to run the complete screening protocol described herein—including spheroid initiation, drug treatment and determination of the analytical end points (spheroid integrity, and cell survival through the acid phosphatase assay)—is about 170 h. Monitoring of spheroid growth kinetics to determine growth delay and regrowth, respectively, after drug treatment requires long-term culturing ($\geq$14 d).

INTRODUCTION

Over the past several years, various types of 3D culture systems have garnered much attention and gained increased recognition as important research tools. This trend has been illustrated, among others, in Alison Abbott's 2003 *Nature* report entitled 'Cell culture: biology's new dimension', which particularly emphasized the basic necessity for such systems before turning to whole-animal studies, for both basic research and therapeutic development[1]. Examples of 3D culture systems in use that show intermediate complexity reflecting particular aspects of tumor tissues include multilayer cell systems. These have been applied, for example, to study phenomena, such as drug transport and binding, therapy resistance and cell invasion. Matrix-embedded 3D cultures are increasingly applied to investigate differentiation, migration and invasion processes of tumor cells triggered by extracellular matrix compounds. Hollow-fiber-based approaches and *ex vivo* cultures of pieces or slices from tumors are also to be mentioned as advanced 3D culture systems but are not yet sufficiently well standardized and/or depend on the supply of primary tumor tissue, which can be challenging to obtain and limits routine application[2,3]. Continuing progress in testing natural and artificial matrices as well as 3D scaffolds, e.g., for tissue engineering purposes, has resulted in a number of critical improvements in reproducibility, ease of use and reliability of 3D model systems, with many obvious applications especially in cancer research. Some approaches have been discussed earlier with particular focus on the multicellular spheroid system as one of the models that has been characterized sufficiently well to say with confidence that it simulates the pathophysiological milieu in a patient tumor showing similar therapy responses[4–7].

Multicellular spheroids are probably the most classical approach for 3D culturing, and multiple review articles throughout the past three decades have highlighted the potential of this model system in cancer research and treatment[2,7–10]. Early investigations in the 1970s not only triggered the study of basic biological mechanisms in multicellular tumor spheroids (MCTSs), such as the regulation of tumor cell proliferation, differentiation and cell death processes, but also initiated the progressive entry of the MCTS model into various new fields of therapeutic interest. Today, there is an enormous body of literature on multicellular spheroids used in therapy-oriented studies, far too numerous to be discussed at length herein. However, it is worth noting that many of these studies have demonstrated the particular power of MCTSs to gain insight into therapeutic problems associated with metabolic and proliferative gradients, such as the altered responsiveness and effects of chronically hypoxic tumor cells, and the importance of 3D cell–cell and cell–matrix interactions, e.g., in radio- and chemoresistance[10,11–15]. In fact, tumor cells grown as 3D structures can acquire some type of clinically relevant multicellular resistance to apoptosis-inducing drugs that may mimic the chemoresistance found in solid tumors[16–19]. Accordingly, experts in the field have proposed to include MCTSs as mandatory models in major programs for drug screening and development and frequently alluded to the rationale for using MCTSs in antitumor drug testing[2,7,20].

In brief, MCTSs resemble avascular tumor nodules/micrometastases or intervascular regions of large solid tumors with respect to micromilieu, volume growth kinetics and some histomorphological features. They reestablish morphological, functional and mass transport properties of the corresponding tissue *in vivo*, with tumor cells restoring an *in vivo*-like differentiation pattern due to the appropriate 3D extracellular matrix (ECM) assembly, complex

cell–matrix and cell–cell interactions and authentic pathophysiological milieu conditions. With increasing size, inward proliferation and oxygen/nutrient gradients are observed[21], as well as a potential accumulation of catabolites in central regions, highly reminiscent of poorly vascularized areas in solid tumors. All these features affect cellular RNA and protein expression, the distribution and function of biomodulators and also the penetration, binding and bioactivity of therapeutic drugs and drug candidates. According to literature data, we expect many drug candidates to lose efficacy in the 3D pathophysiological environment[3,8,15,20]. Here, spheroids will be a tool for negative selection and could (i) contribute critically to a reduction in animal testings and thus to economical savings and (ii) also become a powerful model to optimize drug candidates for enhanced tissue distribution and efficacy. On the other hand, there is also experimental evidence that some drugs may exclusively be effective in 3D but not 2D culture, as has been seen in some target-specific treatment modalities, often with the molecular target being expressed only or particularly in a 3D environment[18,22–29]. Of course, drug candidates failing to show efficacy in classical monolayer test assays but showing up active in a spheroid-based screen pose an interesting challenge for novel drug development offensives.

To use the spheroid model as a supplement to monolayer-based assays with well-controlled intermediate complexity for advanced drug testing to better estimate *in vivo* antitumor efficacy[2,20,30], it is important to assure that the pathophysiological features of interest are indeed reflected. Some of these considerations, including the advantages and also the limitations of our protocol, are discussed further in the Experimental design. In general, implementation of the model into primary drug testing routines requires an experimental design that guarantees that spheroids cultured from the same cell type under the same external conditions are essentially identical in structure, morphology, microenvironment and cellular physiology. To allow the efficient generation of a few up to several thousands of individual, identical cultures for screening purposes, for the performance both of single assays and multiple independent assay series, a well-defined geometry is of course mandatory. An additional advantage of uniform geometry is the potential to relate structure to function, correlate spatial distributions or perform theoretical analyses[2,20,30]. Once data mining becomes feasible and necessary, on the basis of the accumulation of efficacy data for reference substances and drug candidates, respectively, this will become both a challenge and an opportunity for optimizing drug design strategies, but this is clearly beyond the scope of this protocol. It is rather our intention to provide a list of critical considerations when establishing spheroid monocultures for therapy testing, present routine protocols with some technical improvements from our laboratory to monitor parameters of interest for an initial 'spheroid-based screen'[3,7] and caution against some of the basic and most frequently encountered pitfalls.

Experimental design

Although it may be impossible to achieve a general standardization of spheroid culturing and analysis for all experimental settings, the easy-handling protocols presented herein for highly reproducible spheroid culturing, volume analysis and cell viability assessment are expected to essentially contribute to the establishment of a 'spheroid-based screen' and to encourage scientists and the pharmaceutical industry to consider spheroids as part of the standard repertoire for drug testing. However, before going into further detail with respect to the protocols applied in our laboratory, we intend to discuss some points of interest that have often been ignored but are critical when setting up spheroid-based assays. We do not intend to give a comprehensive review on different spheroid culture techniques nor will we discuss the more complex approaches, such as spheroid coculture systems, which have been established over the past 15 years to more closely resemble cellular heterogeneity in tumor tissues and which have included cell types as diverse as stromal fibroblasts, immune cells and endothelial cells[7,9,31–35]. These are indeed highly relevant and interesting model systems for academic work and should be considered for experimental drug testing. But the need to generate spheroids with uniform fractions and distributions of the different cell types as a prerequisite for a drug screening platform is a demanding challenge, and rapid, easy-handling analytical tools are not yet available[2,7,9]. Therefore, this protocol focuses on the culture, treatment and analysis of multicellular spheroid monocultures from established, commercially available human tumor cell lines and on routine approaches to evaluate spheroid formation capacity for noncommercial tumor cells or clones of interest. Some relevant considerations for the design of a large-scale spheroid-based drug screen are discussed.

Tumor cell type of interest. The spheroid model is not equally relevant for all malignant diseases and scientific questions. For some types of nonsolid cancers, such as leukemia, lack of relevance of the spheroid monoculture model seems obvious, at least with respect to various pathophysiological parameters. Drug resistance phenotypes resulting from cell adhesion phenomena, however, may even be reflected for hematological malignancies[36]. For other tumor entities, specific questions are to be raised. With respect to melanoma, e.g., skin culture models are clearly the better approaches to reflect tumor cell behavior at the primary tumor location[37–39], but spheroids may well reflect metastatic growth. They are preclinical models of avascular metastases and—provided the researcher is aware of the relevant limitations—they can prove useful for studying the nature of metastatic disease. Furthermore, they resemble intervascular microregions in carcinomas and sarcomas and have also been widely used as a model for brain tumors, in particular gliomas and glioblastomas. We recently tested all epithelial tumor cell lines of the NCI-DTP 60 cell-line panel for spheroid formation under identical conditions (**Table 1**). An extended list with other epithelial cell lines grown as spheroids, in addition to the ones tested by us, has been reported earlier[7].

Neither all primary tumor cells nor all established cell lines are capable of forming spheroids. Spheroid formation capacity has to be evaluated independent of the spheroid culture technique. Some tumor cells form spheres spontaneously in the absence of attachment to another substrate, even under stirred conditions. For those that do not aggregate, a period of culturing under steady-state conditions is recommended in standard approaches, such as the liquid overlay method. If a particular cell line does not form spheroids using standard spheroid culture technologies, including liquid overlay (for review, see refs. 7,37), but its use is nevertheless essential, the addition of ECM compounds, Methocel or reconstituted basement membrane according to Korff and Augustin[40] or Ivascu and Kubbies[41] can be considered. Although such 'artificial' matrices may allow obtaining spheroids from nonadherent and

TABLE 1 | Human epithelial cancer cell lines used in the NCI-DTP 60-cell line screen that form spheroids in liquid overlay 96-well plates and that are adequate for drug screening purposes under identical standard culture conditions as detailed in PROCEDURE.

Tumor entity	Cell line	Maximum spheroid diameter (μm)	Supplier
Colon	DLD-1[a]	750–850	ATCC
	HCC2998	600–700	NCI
	HCT-15[a]	500–600	ATCC
	HCT-116	>1,000	ATCC
	HT29	>1,000	ATCC
	KM12L4A	>1,000	NCI
	KM20L2[b]	~1,000	NCI
Breast	BT549	No growth after formation	ATCC
	Hs578T	No growth after formation	ATCC
	MCF-7	Not definable[c]	ATCC
	T47D	850–950	ATCC
	? MDA-MB-435[d]	>1,000	NCI
	? NCI/ADR^{RESe}	550–650	NCI
Ovary	OVCAR-8	800–900	NCI
	SKOV3	600–700	NCI
Prostate	DU-145	No growth after formation	ATCC
Kidney	786-0	No growth after formation	NCI
	CaKi-1	750–850	ATCC
	SN12C	900–1,000	NCI
	SN12K1	Not definable[c]	NCI
	UO-31	No growth after formation	NCI
Lung/NSCLC	A549	~1,000	ATCC
	HOP-62	No growth after formation	NCI
	NCI-H23	>1,000	ATCC
	NCI-H226	No growth after formation	ATCC
	NCI-H460	800–900	ATCC

ATCC, American Type Culture Collection. NCI, National Cancer Institute. [a]DLD-1 and HCT-15 have the same genetic origin but different chromosome changes[89]. [b]KM20L2 is a variant of HT29[90]. [c]Spheroids grow, but increasingly irregular surface impede correct volume analysis. [d]MDA-MB-435 breast origin is questioned as cells express melanocyte-specific genes[91,92]. [e]NCI/ADR^{Res} cells were recently identified to be derived from the ovarian cell line OVCAR-8[93].

eventually highly metastatic tumor cells, the occurrence of matrix-driven alterations in growth, expression profile and behavior of the cells, including drug response, must be taken into consideration. However, such effects have not been systematically studied, and their *in vivo* relevance requires further examination. We highly recommend that all spheroid types in a screen should be grown under identical conditions. The primary 'spheroid-based screen' described herein was designed to not include any artificial supplements except for standard conditioned media and the coating to provide a nonadherent surface for liquid overlay.

Similar to the case with monolayer cultures, many spheroid types are kept typically in different cell type–specific media to assure reasonable spheroid growth and maintain viability. This is, of course, undesirable for high-throughput screening purposes and also with respect to some pathophysiological features that should continue to be reflected properly in the model. Just as an example, differences in glucose supplementation may alter survival and/or drug sensitivity of cells under hypoxic conditions. Thus, we recommend the physiological range of 1 g liter^{-1} (5 mM) glucose. It is also clear that some conditions cannot be mimicked well *in vitro*. However, within and between screens, the conditions should not vary for the cell lines used, as this would clearly complicate data analysis and interpretation. In our experimental setting, we have adapted all cell lines of interest to growth in Dulbecco's modified Eagle medium (DMEM) supplemented with 10% (vol/vol) fetal calf serum (FCS).

Spheroid size and culture time. The physiological state of spheroids clearly depends on the spheroid size, the individual and cell type–specific behavior of the tumor cells, the cell density within the spheroid and also directly or indirectly on the culture time. We intended to establish a spheroid-based screen with clear pathophysiological gradients but without central necroses at the onset of treatment. Owing to literature data and our own experience, a 4-d initiation interval for spheroid formation seemed reasonable and was found to reproducibly create spheroids of different cell types under identical culture conditions, reaching a standard size of 370–400 μm after 96 h of incubation at the onset of treatment. The culture of small spheroids with a size of up to 200 μm is frequently carried out for drug testing[42–45] and may indeed be sufficient to reflect 3D cell–cell and cell–matrix interactions but is clearly inappropriate when attempting to resemble pathophysiological conditions with hypoxic areas in the spheroid center or to develop proliferation gradients[8,30,46,47]. Hypoxia is not only a well-established direct radio- and drug- resistance factor, but it also leads to numerous indirect effects in tumor cells by modulating expression patterns, e.g., of HIF-1(α)-regulated genes. For example, it has been shown that growth of human breast cancer, human melanoma and murine breast cancer cell lines as multicellular spheroids lead to a reproducible downregulation of various DNA mismatch-repair genes[48,49], an effect that may also be directly triggered by hypoxic conditions[50]. In spite of using spheroids with a size that is sufficient to develop hypoxia in the center, approaches using small spheroids cultured under hypoxic conditions may thus be considered, keeping in mind of course that oxygen deficiency is only one of a number of pathophysiological parameters with therapeutic relevance. Large spheroids with a diameter between 500 and 600 μm develop central secondary necroses, which may be desired for some drug testing approaches but can be problematic in others. How relevant secondary necrosis is has to be determined for the intended application and for the particular tumor entities *in vivo*—see, e.g., the development of the so-called Comedo necroses in breast tumors. The possibility that such secondary necroses—both *in vitro* and *in vivo*—may develop through apoptosis has to be kept in mind as well[20,22,51].

Short-term cultures may not be as densely packed as those that formed over a longer period, they may not have endured lag phase after dissociation and seeding or may not yet express the entire authentic 3D pattern, e.g., with respect to extracellular matrix distribution and cell–cell/cell–matrix interactions[52]. Also, they may not show the same degree of chronic nutrient-deficiency characteristics. Molecules of interest should thus be carefully checked when short-term cultures of <48 h are used for testing.

Culture technology and treatment modalities. Easy and rapid handling of both spheroid culturing and analysis are a condition for

integration of this model system into routine drug testing. The various techniques for spheroid culturing have been described earlier, emphasizing their individual advantages and disadvantages[7,8,10,37]. It is noted that the spinner flask technique remains the most appropriate for large-scale culturing and for maintaining spheroids under optimal supply conditions over a long period of time. One has to acknowledge, however, that rotating culture systems require relatively high quantities of media, conflicting with the usual demand for minimum amounts of new drug candidates to be applied in a drug test system. It may thus be necessary to transfer the spheroids to stationary spheroid culture systems, not only during drug exposure, but also for determining some of the analytical parameters, such as spheroid volume growth. Such transfer would not only disturb the cultures following treatment but also renders individual spheroid monitoring impossible.

Stationary culturing technologies include the growth of spheroid cultures in nonadherent dishes, 96-well plates or as hanging drops. Whereas the first approach results in the formation of multiple spheroids with a broad size range requiring further sorting and is thus not recommended for screening, the 96-well approach allows monitoring and manipulation of single and uniform spheroids. The hanging drop method is comparably sufficient, but here drug treatment would require spheroid transfer that is counterproductive to large-scale screening. Problems with stationary culturing are primarily due to the more diffusion-limited conditions compared with rotary systems that affect the supply of nutrients and the pathophysiological situation in the spheroids throughout growth but may also alter drug distribution. The implementation of rotating platforms for 96-well plates might be useful to reduce this problem. Other critical points specifically relevant for drug testing in stationary cultures that may complicate interpretation of drug treatment studies have been discussed earlier[7]. Not surprisingly, drug treatment itself can affect the pathophysiological behavior, e.g., metabolic activity, of the cells, leading to secondary effects due to internally induced alterations in the nutrient environment. Such effects may be more pronounced in stationary than in stirred conditions. However, it has been speculated that similar alterations do occur in solid carcinomas due to their leaky, irregular and tortuous vascular system. In high-throughput test settings, some of the limitations of stationary culturing may be inevitable to minimize the amount of drug required. Owing to the need for analyzing and monitoring individual spheroids before and after treatment and to be able to apply small amounts of drugs, we chose the well-established liquid-overlay 96-well plate approach[7,37,53] to set up the spheroid-based screen protocol.

At present, none of the commercially available 96-well plates guarantees entirely reproducible spheroid culture for routine applications. We are continuously testing new plates from various distributors and manufacturers; any test plates are welcome in our laboratory. However, for now, plates with nonadherent surfaces are prepared routinely before spheroid culturing. Different coating strategies are described, such as the treatment of round-bottomed wells with 0.5% (wt/vol) poly-hydroxyethyl methacrylate (poly-HEMA) in 95% ethanol[41,54,55]. Here, a centrifugation step to center the cells following inoculation may be advantageous for adequate spheroid formation. In our laboratory, the quality and reproducibility of spheroid formation and growth was still superior when using Agarose-coated flat-bottomed wells. This may be due to individual handling, the poly-HEMA batches available or other variables. Individual, small-scale testing of poly-HEMA versus agarose coating might, however, be useful for special applications or if problems with certain cell lines or systems occur. Agarose diluted in medium forms a semisolid, nonadherent, concave surface that has proven to be appropriate for liquid overlay spheroid culturing more than 20 years ago[53]. It is hypothesized that the semisolid agar surface provides slightly better supply conditions than the bottom of a (coated) round-well plate, but this is still awaiting clear experimental evidence. *Note*: do-it-yourself coating of plates is obligatory for spheroid culturing, and coated plates should/can only be stored for a limited time (see also instructions below).

Analytical end points. Many basic and complex methods have been used for the analysis of MCTSs, be they viable, fixed or dissociated[2,7,9]. Today, all modern analytical tools, including molecular analyses, can be adapted to spheroid culture and may be considered if the analytical end point in a comparable monolayer system—such as a critical up- or downregulation of a particular gene, set of genes or protein—is well established. Colony formation assays to verify clonogenic survival are an established end point to verify drug efficacy and radioresistance in monolayer cells and cultures, respectively. It has, however, become evident that the cell preparation protocol is a critical determinant for the analytical power of this end point. Accordingly, clonogenic survival assays have also been performed with single cells isolated from spheroids, e.g., following selective dissociation[56–61], but such experimental setups are time intensive, require large amounts of spheroids and are thus not suitable for an initial spheroid-based screen. In addition, artificial cell loss due to the more difficult dissociation procedure for 3D cultures, in particular after drug exposure, may become a major problem. Thus, the first spheroid-based screen to evaluate drug efficacy on a routine basis in our laboratory has been designed to cover the analytical end points: spheroid integrity, cell integrity and regrowth following treatment.

Spheroid integrity can easily be visualized by (rapid) phase-contrast imaging, which is also the basis for recording spheroid volume growth kinetics. We have semiautomated this setting for single spheroid monitoring according to a protocol given below. As spheroid cell detachment directly after treatment may not necessarily result from (total) cell destruction and vice versa, microscopically intact spheroids may as well contain membrane-defect cells; there is no strong argument against the analysis of spheroid volume growth as a function of time. Indeed, spheroid growth delay is one of the supposed end points of interest that can most easily be determined.

Various protocols have been used in the literature to calculate spheroid growth delay. Approaches range from linear and nonlinear correlation analyses of the spheroid volume kinetics considering defined spheroid volume end points to the pure recording of time delay for spheroid regrowth after treatment[62,63]. The variable, nonuniform analysis in past reports has resulted in a dispute over the term 'growth delay.' On the basis of the spheroid diameter of 370–400 μm at the onset of drug treatment (average starting volume V_{d4}: (2.7–3.4) × 10^7 μm^3), our setting includes the documentation of the time required to reach five times V_{d4}, with the growth delay being calculated as the average time difference between treated and nontreated control spheroids. As spheroids after treatment may not show 'normal' tumor growth kinetics, e.g.,

according to a Gompertzian or equivalent function[64–66], we do not routinely perform complex correlation analyses but record the first day of the cultures to have a mean spheroid volume of $\geq 5 \times V_{d4}$ as rapid estimate. This is useful if, as in the case of new drug candidates, pronounced but not minor effects are to be assessed. In addition, the individual spheroid regrowth is recorded, and the proportion of spheroids to reach $5 \times V_{d4}$ is monitored as a function of time. This approach allows estimation of a 50% spheroid control concentration or dose according to the tumor control dose (TCD_{50}) known from irradiation experiments.

Spheroid volume (re)growth is a primary analytical end point. However, it requires long-term culturing, and it is desirable also to have a more immediate measure for cell survival directly after treatment. We have recently established an easy-handling protocol to use the acid phosphatase assay (APH) for cell integrity and viability assessment in single spheroids[3]. The assay is simple, rapid and high-throughput compatible, as it does not require spheroid dissociation. It has been described to be linear and highly sensitive over a large cell concentration range for two well-established colorectal cancer spheroid types, and the results can directly be compared with respective data from monolayer cultures using the same assay. Similar systematic experiments for other simple assays are not documented in the literature, although various groups have applied cell viability or cytotoxicity assays in spheroids[42,67,68]. As we found several of the classical cell viability and cytotoxicity assays not to be applicable to spheroid cultures with varying sizes, we highly recommend to not blindly apply any monolayer assay system but to check the validity of the assay of choice or to use the APH approach described herein. Thymidine incorporation assays may also be useful, as they primarily reflect proliferative activity, but were not considered due to the more complex handling of radioactive material. In our laboratory, IC_{50} values estimated from dose-response curves determined through APH cell viability assessment are used as one analytical end point for drug testing.

The capacity for spheroid outgrowth in 3D matrices or on adherent, ECM coated or noncoated surfaces, has been described previously as an interesting parameter to describe the migratory behavior of spheroid cells[69,70]. However, this is valid only if short incubation intervals of less than one cell cycle are considered or if cell cycle progression is chemically inhibited. Unfortunately, the latter may interfere with drug efficacy and should be avoided. Therefore, the approach is particularly useful only for rapidly migrating cells, e.g., in glioma or glioblastoma spheroids[70]. We have established a high-throughput compatible process to transfer and center single spheroids from agarose-coated into ECM-coated 96-well plates and to semiautomatically analyze spheroid outgrowth. However, for many but not all colorectal cancer spheroid types, outgrowth is seen exclusively over a longer period of time (3–5 d), which does not allow clear discrimination of the effects of a drug on cell adherence, migration or proliferation. The test parameter 'outgrowth' is thus not considered as a primary analytical end point for routine monitoring in the spheroid-based screen and will not be discussed further in this protocol.

Additional methodological considerations. Three types of controls should be considered for a spheroid-based drug test system: (i) spheroid, (ii) treatment and (iii) analytical controls. Spheroid control means that a well-established and characterized spheroid type is routinely included in the experimental setup. We use HT29 spheroids as a standard. Drugs that are already in clinical use either for a specific tumor entity or with broader efficacy can serve as treatment controls. Such drugs may be 5-fluorouracil or irinotecan, e.g., for colorectal cancers, and also paclitaxel, cisplatin or even doxorubicin (adriamycin), which has the advantage of being fluorescent and thus can be useful as a control for drug penetration studies[56,71,72]. Analytical controls, e.g., cell-free medium, dead cell and drug solvent controls and others, are depicted for our specific procedure in the respective paragraphs.

MATERIALS

REAGENTS

▲ CRITICAL The lists provided in this section are based on the materials used in our laboratory. Chemicals and cell culture materials may, of course, also be purchased from other distributors and/or manufacturers.

- Acetic acid 96% (Merck KGaA, cat. no. 1000621000) ! CAUTION Flammable, toxic.
- Agarose (Sigma-Aldrich Chemie GmbH, cat. no. A9539-100G) ▲ CRITICAL Use of other agaroses may cause problems.
- Dimethyl sulfoxide (DMSO; Merck KGaA, cat. no. 317275-100ML) ! CAUTION Hazardous; avoid contact with skin and eyes.
- DMEM (PAN Biotech GmbH, cat. no. P04-01550)
- Electrolyte solution (Casyton, Schärfe System GmbH, cat. no. 43001)
- FCS (PAN Biotech GmbH, cat. no. 3302-P250922) ▲ CRITICAL Serum quality affects spheroid formation and growth and should be routinely tested! Serum may interfere with the APH signal ($n \geq 20\%$ serum).
- ImmunoPure *p*-nitrophenyl phosphate, disodium salt (Pierce, cat. no. 34045)
- Sodium hydroxide (Merck KGaA, cat. no 567530-250GM) ! CAUTION Corrosive, wear suitable gloves and eye/face protection.
- Sodium acetate 3 M, pH 5.2 (Quality Biological Inc., cat. no. 351-035-061)
- Penicillin/streptomycin 1,000 U pen./10 mg strep. per ml (PAN Biotech GmbH, cat. no. P06-07100)
- Phosphate-buffered saline without Ca^{2+}, Mg^{2+} (PBS; PAN Biotech GmbH, cat. no. P04-36500) ▲ CRITICAL For some steps, Ca^{2+}/Mg^{2+}-free conditions are required, e.g., to avoid cell clumping.
- Triton X-100 (Sigma-Aldrich Chemie GmbH, cat. no. X100-100ML) ! CAUTION Harmful/dangerous for the environment; wear suitable gloves and eye/face protection. ▲ CRITICAL Triton X-100 of different manufacturers may vary with respect to cell kill.
- 0.5% (wt/vol) trypsin/0.2% (wt/vol) ethylenediaminetetraacetic acid (EDTA) solution (PAN Biotech GmbH, cat. no. P10-024020)

EQUIPMENT

▲ CRITICAL It is noted that there is a clear difference in the configuration required for laboratories using spheroids for primary but large-scale drug testing, as is the focus herein, versus those most suitable for addressing basic research-driven questions. Automated phase-contrast imaging, e.g., is not required for spheroid work per se but should be available for a spheroid-based drug screening platform. Some equipment can be substituted by other systems, e.g., pipetting and microscope apparatuses as well as application software. We have added information on the particular use of the specific equipment for our protocol to allow potential and sufficient substitution in the reader's laboratories.

- Autoclave: tabletop autoclave Model DC2002 (Biocare Medical) (see EQUIPMENT SETUP)
- Beaker system from either one-way material or reusable glassware (e.g., Schott; see EQUIPMENT SETUP; **Fig. 1**)
- Cell analyzer: cell counter Casy 1 Model 1 TTC (Schärfe System GmbH)
- Cell culture flasks T75 and T175 (Greiner Bio-One GmbH, cat. nos. 658175 and 660175)
- Cell culture plates Microtest, 96-well, flat bottomed (Becton Dickinson GmbH, cat. no. 353075; see EQUIPMENT SETUP)
- Centrifuge Megafuge Model 1.0 or Multifuge 1S-R (Heraeus Sepatech GmbH)

- Centrifuge Varifuge Model 3.2RS or Biofuge stratos (Heraeus Sepatech GmbH; see Step 9B(ii))
- CO_2 incubators, such as Heraeus Model T 6120 and Hera cell 150 (Heraeus GmbH)
- Clean benches, such as Laminair 2472S/HBB 2448 and Hera safe KS18 (Heraeus GmbH) or Holten 2010 1.2 (Holten) ▲ CRITICAL Required for sterile cell culture handling.
- Microplate Readers, e.g., the Emax Precision Microplate Reader (Molecular Devices Corporation) or Fusion Universal Microplate Analyzer (Packard; see Steps 9A(vi) and 9B(viii))
- Microscopes: Axiovert 200 microscope equipped with an AxioCam MRc camera (Zeiss AG, cat. no. 426508-9901-000) and an Axiovert 200 M microscope equipped with an AxioCam MRm camera (Zeiss AG, cat. no. 426509-9901-000; **Fig. 2**)
- Nitrogen tanks, such as the Model GT 75 l (Air Liquide GmbH) or the Apollo Cryosystem (KGW Isotherm)
- Pipettor, AccuJet (Brand GmbH + Co KG, cat. no. 26300)
- 5-, 10- and 25-ml polypropylene (PP) pipettes (BD Falcon, cat. nos. 357543, 357551 and 357525)
- Pipettor, 8-channel (Brand GmbH + Co KG, cat. no. 703608)
- 100-µl Ultratips (Greiner Bio-One GmbH, cat. no. 739296)
- 300-µl Plastibrand tips (Brand GmbH + Co KG, cat. no. D-286-3)
- Pipettor, electronic multichannel Finn Pipettus Biocontrol (50–1300 µl)
- Extra volume tips (100–1,300 µl; StarLab, cat. no. I1012-2000)
- Pipettor, Multipette plus or multipette x-stream with 5-ml combi tips (Eppendorf GmbH, cat. no. 0030069.455; see EQUIPMENT SETUP; **Fig. 1**)
- SerialMate automated multichannel pipetting system (Thermo Fisher Scientific Inc.; see Step 4; **Fig. 2**)
- Tubes: 15- or 50-ml PP tubes (Greiner Bio-One GmbH, cat. nos. 188271 and 210261)
- Cryo tubes (Cryo.S, PP, sterile; Greiner Bio-One GmbH, cat. no 122261)

REAGENT SETUP

Standard medium Dulbecco's modified Eagle's medium with phenol red containing 1 g liter^{-1} glucose, 1% (wt/vol) sodium pyruvate, 1% (wt/vol) L-glutamine and 3.7% (wt/vol) $NaHCO_3$, supplemented with 100 U ml^{-1} penicillin, 100 µg ml^{-1} streptomycin and 10% FCS is used as standard medium for routine cell and spheroid culturing. Standard medium can be stored at 4 °C for up to 2 weeks.

Trypsin/EDTA working solution Phosphate-buffered saline is applied to dilute the trypsin/EDTA stock solution to a final concentration of 0.05% (wt/vol) trypsin and 0.02% (wt/vol) EDTA. The working solution can be stored at −20 °C for up to 1 year.

Drugs and drug candidates Prepare appropriate stock solutions of drugs and drug candidates, respectively, and store at conditions required to keep optimum drug activity. In our first standard spheroid-based screen, final drug concentration ranged from 0.01 to 200 µM, but some drug candidates are efficient at much lower concentrations. For most but not all drugs in our laboratory, 100 mM stock solutions in DMSO and storage at −20 °C for up to 2 weeks are suitable.

APH assay buffer The assay buffer to assess APH activity contains 0.1 M sodium acetate (3 M stock solution, pH 5.2) and 0.1% (vol/vol) Triton X-100 in deionized/destilled H_2O and can be stored at 4 °C for up to 4 weeks. The substrate solution is prepared by supplementing the assay buffer with 2 mg ml^{-1} ImmunoPure *p*-nitrophenyl phosphate (final pH 4.8) immediately before use. ▲ CRITICAL The substrate solution should always be freshly prepared and not be exposed to light.

EQUIPMENT SETUP

Tumor cells Various epithelial tumor cell lines of different origin are known to form spherical cultures[7]. Not all of these can be applied in a spheroid-based screen. Diverse considerations have been discussed above. The first spheroid-based drug screen for multiple cell lines has been designed to exclusively monitor drug efficacy in colorectal cancer cell spheroids. All of these lines are commercially available (**Table 1**), can be cultured as monolayer and spheroid cultures in standard medium and transferred using the same trypsin/EDTA working solution. HT29 and HCT-116 are the routine cell lines in our platform. All stocks have been tested to be free of mycoplasms, are frozen in a 90% FCS plus 10% (vol/vol) DMSO solution and are stored in liquid nitrogen for subsequent reculturing.

Agarose-coated 96-well plates Add 0.15 g of agarose to 10 ml of DMEM (1.5% (wt/vol)) in appropriate beaker, seal with aluminum foil or lid and autoclave for 20 min at 120 °C, 2 bar. Open autoclave at ~90 °C and transfer beaker to sterile workbench; do not allow agarose to cool down and solidify. It is recommended to keep beakers with agarose in a preheated waterbath on heating plate at about 60 °C. Add 50 µl to each well of a 96-well microtiter plate (flat bottomed) under sterile conditions using a manual precision dispenser. The agarose solidifies within seconds to minutes. A volume of 50 µl agarose is appropriate to produce a concave surface and is a convenient choice to allow the addition of 200 µl of cell suspension and supernatant, respectively. Let plates with agarose cool down to room temperature (~20 min) and repack plates. Plates can be used for up to about 10 d after preparation if hermetically sealed, stored at room temperature and protected from light. ▲ CRITICAL Amounts less than 50 µl may not entirely cover the surface before solidifying.

Figure 1 | Tools for routine preparation of agarose-coated 96-well plates. Self-designed reusable beaker and rack system (upper panel), to be used in a commercial table autoclave (middle panel) and transferred into a preheated waterbath for agarose dispension under sterile condition (lower panel). The system shown allows the preparation of 30 plates at a time that are hermetically sealed after cooling off.

Phase-contrast imaging: AxioVision 4.5 software In collaboration with Zeiss AG, we established semiautomated measurement protocols to determine diameters and volumes from spheroid phase-contrast images using specific modules in the AxioVision 4.5 software (Zeiss, Germany). The following parameters are recorded: spheroid area, mean spheroid diameter, spheroid volume, minimum diameter, maximum diameter, circularity and image name.

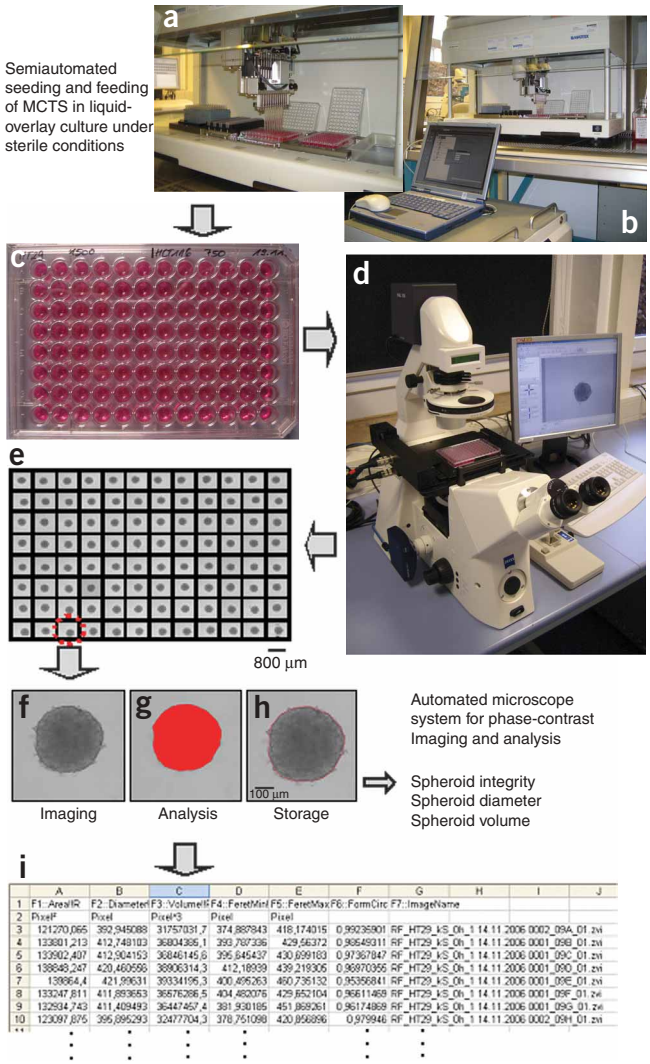

Figure 2 | Routine spheroid analysis includes phase-contrast imaging at days 4 and 7 (before and after drug treatment) and every 48 h thereafter. (**a**–**c**) 96-well plates with spheroids are prepared and (**d**) transferred onto the automated stage of a Zeiss Axiovert 200/M (photo documentation). (**e**,**f**) Phase-contrast images are taken with a ×10 or ×5 objective. Automated documentation of 96 spheroids requires <10 min without autofocus and about 12 min with autofocus, respectively. (**f**,**g**) Spheroid analysis is performed semiautomatically through implemented, image-processing algorithms in the AxioVision 4.5 Software (Zeiss), which allows reliable and reproducible area selection to determine spheroid diameter and volume. (**i**) Routinely generated data tables contain the relevant morphometric information (see Step 6 of PROCEDURE).

PROCEDURE

Spheroid initiation ● TIMING Working time 1–2 h, incubation time 96 h

1| Thaw tumor cells routinely from frozen stocks and subculture for >1 and <20 passages (before spheroid initiation). Use 'standard medium' for routine culturing[3]. Keep cultures in humidified atmosphere with 5% CO_2 in air at 37 °C.

2| Prepare single-cell suspensions by mild enzymatic dissociation using a trypsin/EDTA solution[9]. Transfer stock cultures every 3–4 d by seeding appropriate numbers of cells of (0.5–1) × 10^6 (depending on cell type and doubling time) into T75 culture flasks. Avoid repeated dissociation of monolayers within less than 2 d.

3| To generate spheroids of 400-µm diameter at day 4 after inoculation in liquid overlay culture[37,53], dilute dissociated cells from stock cultures to appropriate concentrations in standard medium, e.g., 7,500 cells ml^{-1} for HT29 and 3,750 cells ml^{-1} for HCT-116 human colon carcinoma cells.
▲ CRITICAL STEP For each tumor cell line, the cell number needed to create spheroids of 370–400 µm in diameter at day 4 after initiation (see Step 6) has to be determined in preliminary tests using appropriate dissociation means to produce single cell suspensions. In our setup, spheroid formation is routinely checked by phase-contrast microscopy for cell concentrations ranging from 2.5 × 10^3 to 6 × 10^4 cells ml^{-1} (as described in Step 6). A representative example of one cell type from the NCI-DTP 60 cell line panel tested is shown in **Figure 3**. Reproducibility is then checked twice, 3D sphericity is evaluated, and spheroid characteristics of interest, e.g., the number of cells per spheroid, at the respective diameter are documented.

4| Use a manual eight-channel pipettor or an automated multichannel pipetting system, such as the SerialMate to transfer 200 µl of the cell suspension into each well of an agarose-coated microtiter plate (1,500 HT29 and 750 HCT-116 cells per well, respectively). Application of an automated multichannel pipetting system (**Fig. 2**) may optimize spheroid formation by reducing variability due to individual handling during seeding. The standard deviation (s.d.) of HT 29 spheroid diameters at day 4 after seeding is reproducibly below 5% in one 96-well plate and one experimental 96-well plate series, respectively, and less than 10% between different experiments.
? TROUBLESHOOTING

5| Incubate plates for 96 h in a humidified atmosphere with 5% CO_2 in air at 37 °C.
▲ CRITICAL STEP Avoid agitation during initiation interval.
? TROUBLESHOOTING

6| After 96 h of incubation (day 4 after intiation of spheroids), image each well of the 96-well plate with a phase-contrast microscope using a ×10 or ×5 objective to monitor and analyze spheroid integrity, diameter and volume. An automated Zeiss Axiovert200/M-based system is used for this purpose in our laboratory. Spheroid analysis is performed through image processing algorithms implemented in the AxioVision 4.5 Software (Zeiss), which allows reliable and reproducible area selection to determine spheroid diameter and volume (**Fig. 2**). Routinely generated data tables contain the following morphometric

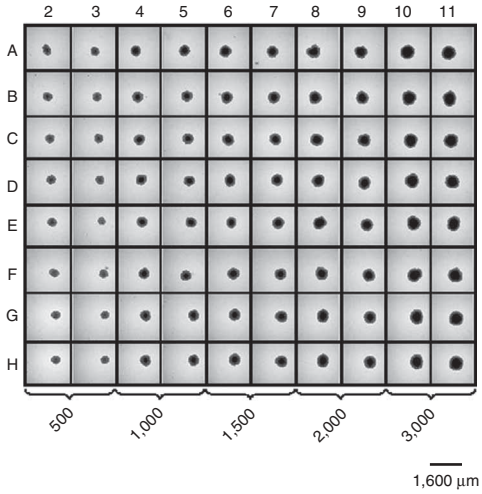

Figure 3 | Routine monitoring of spheroid formation capacity and establishment of the spheroid initiation protocol for one representative cell line. Phase-contrast images of MCTSs formed in liquid overlay from dissociated, exponentially growing NCI-H460 lung carcinoma cells after a 96-h initiation interval in agarose-coated 96-well microtiter plates. The seeding density was between 0.5×10^3 and 3.0×10^3 (from columns 2–11) per well in 200 µl of serum-conditioned DMEM standard medium; original magnification, ×5 objective. Wells in columns 1 and 12 contained medium only and were not imaged. The concentration to routinely and reproducibly obtain spheroids with a diameter of 370–400 µm is 500 cells per well. The layout refers to the 96-well plate coordinates.

information: spheroid area (area), mean spheroid diameter (diameter), spheroid volume (volume), minimum diameter (FeretMin), maximum diameter (FeretMax), circularity (FormCirc) and image name of the stored image of an evaluated area selection. The image name is based on cell line, date and time of measurement, location on plate and plate number.

Drug treatment ● TIMING Working time 1 h; incubation time 72 h

7| For spheroid and monolayer treatment, respectively, dilute drugs or drug stock solutions in standard medium at 2× final concentration immediately before usage. As reference for nontreated control cells and spheroids, standard medium containing the respective solvent, e.g., DMSO, according to the concentration present in the lowest drug dilution (2 × 200 µM) is prepared.

▲ **CRITICAL STEP** Note that DMSO concentrations of <0.5% are not expected to affect spheroid growth. Slight effects may already be seen at a concentration of 0.5–1%, depending on the cell type and culture condition. A proportion of >1% DMSO in the drug dilution for treatment should be avoided. Other solvents are to be verified. Individual solvent controls for each drug concentrations may be considered.

8| Treat spheroid cultures by replacing 50% (=100 µl) of supernatant with drug-supplemented standard medium using a manual 8-channel pipettor or the SerialMate automated multichannel pipetting system. In parallel, replace medium of untreated reference cells and spheroids with solvent-containing or solvent-free standard medium. In our setup, 8–16 spheroids are treated and analyzed per condition and drug concentration, respectively.

▲ **CRITICAL STEP** Spheroid symmetry (sphericity) should be checked in control untreated spheroids before using a new spheroid type for routine drug testing. In some instances, it may be recommended to also monitor 3D spherical structure following treatment, e.g., if spheroids grow much larger than expected and/or become transparent.

? TROUBLESHOOTING

9| Incubate cultures for a defined treatment interval (in our case for 72 h) in a humidified atmosphere with 5% CO_2 in air at 37 °C.

Determination of cell viability using the acid phosphotase assay ● TIMING 2–3 h

10| The APH assay proved useful to determine cell viability in monolayer and spheroid cultures[3]. As we routinely determine drug effects in monolayer cultures in parallel to spheroid cultures, the APH assay procedure for monolayer cells shall also be described herein. The assay procedure differs for monolayer cultures (option A) and MCTSs (option B).

(A) APH assay on monolayer cultures

(i) Prepare monolayer cells for every test as follows: plate 600 exponentially growing monolayer cells in 200 µl of standard medium per well of a 96-well microtiter plate (flat bottomed) and incubate for 4 d in humidified atmosphere with 5% CO_2 in air at 37 °C. Treat monolayer cells according to the instructions for spheroid cultures described in the previous section (Steps 6–8).

(ii) After treatment, wash monolayer cultures by carefully replacing the 200 µl of supernatant with PBS.

(iii) Repeat wash step and add 100 µl of PBS per well.

(iv) Add 100 µl of APH assay buffer to each well and incubate for 90 min at 37 °C in an incubator.

? TROUBLESHOOTING

(v) Following incubation, add 10 µl of 1 N NaOH to each well.

(vi) Measure absorption at 405 nm within 10 min on a microplate reader.

? TROUBLESHOOTING

(B) APH assay on MCTSs

(i) Analyze sphericity, spheroid integrity and diameter of MCTSs grown in liquid overlay for 7 d (initiation period of 4 d plus treatment interval of 72 h), i.e., from Step 10, through phase-contrast imaging before APH assaying.
▲ CRITICAL STEP 10% Triton X-100 in standard medium can be used as ultimate (positive) control to induce complete loss of cell membrane integrity of all cells in structurally intact spheroids with an incubation interval of 2 h before APH assaying.

(ii) Carefully transfer MCTSs and entire supernatant with cells into standard flat-bottomed 96-well microplates with a manual eight-channel pipettor.
▲ CRITICAL STEP Note that APH assays are routinely performed with 8–16 spheroids per condition and treatment modality. Most experiments are repeated twice, except for rapid, preliminary concentration screening. Application of an automated pipettor is envisioned upon assay scale-up.

(iii) Centrifuge for 10 min at RT at ~400*g* to spin down spheroids, clusters and single cells.

(iv) Wash spheroid/cell pellet by carefully replacing 160 µl of the supernatant with PBS.
▲ CRITICAL STEP Be sure not to lose any cell material.

(v) Repeat centrifugation and discard supernatant to a final volume of 100 µl.

(vi) Add 100 µl of APH assay buffer to each well and incubate for 90 min at 37 °C in an incubator.
? TROUBLESHOOTING

(vii) Following incubation, supplement each well with 10 µl of 1 N NaOH.

(viii) Measure absorption at 405 nm within 10 min on a microplate reader.
? TROUBLESHOOTING

Determination of spheroid integrity and volume growth kinetics ● TIMING Working time 1 h per drug every 2 d over a period of ≥14 d

11| Culture spheroids in liquid overlay and treat as detailed earlier (Steps 1–9). For studies on spheroid growth delay/regrowth, replace 50% of the supernatant by fresh, standard medium after the treatment interval and every 48 h thereafter.
▲ CRITICAL STEP To avoid spheroid cell loss or disruption, supernatant cannot be removed completely even after treatment. In most applications, we accept replacement of 50% of the supernatant leading to a 1:2 dilution of the remaining drug and residual drug activity, respectively, which is then consecutively diluted throughout further culturing, i.e., with every medium refreshment. The incubation period is thus not as clearly defined as for the APH assay setting at least for those drugs that are still highly active after 72 h at 37 °C. Approaches to adapt and eventually optimize this setting for semiautomated test routines are discussed, and some basic tests are underway. Sequential treatment is, of course, also feasible but unlikely in a primary screen/test system.

12| Collect phase-contrast images of all individual spheroids before drug treatment (day 4 in culture), after 72 h of treatment (day 7 in culture) and at least every 48 h thereafter either manually or automated, e.g., on a Zeiss Axiovert 200 or automated Zeiss Axiovert 200 M equipped with camera systems and workstations.

13| Monitor and analyze spheroid integrity, diameter and volume semiautomatically at any given time from images taken with ×5 or ×10 objective, respectively, using appropriate software modules, e.g., in the AxioVision 4.5 software (**Fig. 2**).

14| Routinely transfer list of data into worksheet (e.g., in Excel) or specific databank (not yet commercially or freely available) for subsequent spheroid data analysis, and plot mean spheroid volume as a function of time on a semilogarithmic scale to visualize spheroid volume growth kinetics and to evaluate spheroid growth delay after treatment.
? TROUBLESHOOTING

15| As potential analytical end point, determine the time delay and the proportion of treated spheroids versus nontreated spheroids to reach the spheroid volume five times higher than the starting volume at day 4 after initiation ($5 \times V_{d4}$), i.e., spheroid volume at the onset of treatment, and also record the first day of spheroid regrowth following treatment if possible (see also Experimental design)
▲ CRITICAL STEP The spheroid volume $5 \times V_{d4}$ is valid for all spheroid types reaching diameters of ≥700 µm under standard conditions. For some practical reasons not discussed herein, the maximum spheroid volume is a poor analytical end point in liquid overlay culture.
? TROUBLESHOOTING

● TIMING
A time table with day 0 defined as the day of cell seeding for spheroid initiation is given in **Figure 4**.

? TROUBLESHOOTING
Troubleshooting advice can be found in **Table 2**.

TABLE 2 | Troubleshooting table.

Step	Problem	Possible reason	Solution/action
4	Irregular or insufficient agarose coating	Wrong type of agarose	Use appropriate agarose according to instructions
		Agarose solidifies during dispension	Do not allow agarose to cool down below 50–60 °C after autoclaving Transfer and keep beaker with agarose in heated water bath during dispensing process Do not leave agarose in dispensor tip when not dispensing Use new tip if agarose starts solidifying within dispensor tip Use appropriate amount of agarose per surface area to guarantee the formation of a concave agarose surface
		Nonplane surface of workbench	Check and level workbench
5	Inhomogeneous spheroid formation on individual 96-well plates or plate series	Irregular agarose coating	See above
		Unsuitable storage of agarose-coated 96-well microplates	Plates can be stored under various conditions, e.g., at 4 °C in a fridge or at 37 °C in an incubator. We experienced reduced reproducibility of spheroid formation with such approaches and therefore recommend hermetically sealed, light-protected storage at room temperature (20–24 °C). This procedure sufficiently protects against dehydration over the storage period. Another option would be the coverage of agarose with small amounts of medium
		Inhomogeneous inoculation of cells	Always provide optimal single cell suspensions for cell seeding Avoid or get rid of cell doublets and clusters by adapting the enymatic and mechanic means and modalities used for cell dissociation, filter cell suspension through 30–35 μm sterile meshes, and/or use fine needle aspiration Use standardized cell quality assessment settings to guarantee cell viability Exclusively apply cell suspensions from exponentially growing, nonsenescent cells
	Nonreproducible spheroid formation on different 96-well plate series	Serum quality critically affects spheroid formation and growth *Note*: application of serum-free medium is feasible and could enhance reproducibility in cell/spheroid culturing and APH assaying[30] in some approaches	Do not use different batches of serum Check serum quality for spheroid formation and growth before routine use; reserve adequate quantities of the same batch Heat-inactivate serum (56 °C, 20–25 min) even if some of the activity is lost If serum aliquots are frozen for storage, avoid repetitive thawing
		Poor quality of agarose-coated plates	See above
		Poor quality of single-cell suspension for cell inoculation	See above

(continued)

TABLE 2 | Troubleshooting table (continued).

Step	Problem	Possible reason	Solution/action
	Reduced reproducibility of well-established spheroid types	Plates were disturbed during spheroid initiation	Avoid movement and monitoring of plates after cell inoculation for at least 48 h If feasible, use separate incubator for spheroid initiation to elude frequent openings Never slam doors of the respective and adjacent incubators
		Disordered growth of cells in monolayer stock cultures either after thawing or at high passages	Transfer stock cultures at least twice after thawing and before spheroid initiation (see time table, **Fig. 4**) Trash morphologically and/or genetically altered cells and renew stock cultures from the frozen backup Routine cell culture quality assessment, e.g., with cell analyzer system, is recommended
		Poor quality of agarose-coated plates or inadequately dissociated single cell suspensions	See above
		Incorrect incubation conditions or medium supplementation	Check incubator settings and media For large-scale experiments, addition of HEPES as buffer supplement to the medium (10–25 mM) is highly recommended to avoid critical variations in the pH during spheroid monitoring and feeding procedures
	Spheroids in margin wells are smaller	Inhomogeneous incubation conditions (e.g., with respect to humidified atmosphere leading to increased medium evaporation in outer wells)	Check and optimize incubator functions and settings, including water level and CO_2 content
		Eventually, insufficient sealing of agarose-coated plates during storage leading to some quality loss in the peripheral wells	See above *Note*: we found spheroids in the left and right wells (columns 1 and 12) to be more frequently affected than others, although other spheroids in lanes A and H are in line with those on the rest of the plate. At present, our strategy for drug treatment is thus to routinely neglect data from spheroids in columns 1 and 12 but to fill these wells with cell suspensions and/or media anyhow
	Formation of irregular, noncircular spheroids	Small particles in medium and/or serum	Check cleanness of beakers and of any other reusable glass or plastic materials Use one-way materials Monitor media and media supplements and filter supplemented media through sterile filter if required Carefully aliquot heat-inactivated serum to omit solid particles
		Biological variability	See Experimental design. Always check sphericity of new spheroid types not only in phase-contrast images (*x*–*y* direction), but also in *z*-direction, e.g., by individual macroscopic monitoring during manipulation and manual transfer of spheroids and/or through histological processing and sectioning

(continued)

TABLE 2 | Troubleshooting table (continued).

Step	Problem	Possible reason	Solution/action
8	Extreme/critical variation in drug efficacy in spheroids treated with identical drug concentrations	Irregular replacement of supernatant leading to different drug concentrations in parallel wells	Be sure to replace (and to keep) 50% of the original supernatant in all wells, i.e., before the addition of 100 µl of new drug solution, the supernatant kept in each well should be 100 µl
		(Visible) evaporation of supernatant before or during treatment	Check incubation conditions and incubator functions, i.e., water level
		Inappropriate preparation and distribution of drug	Guarantee drug solubility and provide appropriate stock solutions Always start with the lowest drug concentration both when providing the drugs and when feeding the respective spheroids after treatment Use new tips for each concentration In general, perform all experiments according to good laboratory practice (GLP) conditions (or good manufacturing practice; GMP) and provide standard operating procedures
10A (iv), 10A(vi), 10B (vi) and 10B(viii)	Nonspecific APH signal at 405 nm without addition of substrate and/or hydroxide	Autoconversion of PNPP at daylight	Mix buffer/substrate solution immediately and exclusively before use and avoid light exposure
10A(vi) and 10B (viii)	High, inconsistent APH signal in cell/spheroid-free control media	Interaction of serum components and acid phosphatase or PNPP, respectively	Serum concentrations in supernatants of $<1\%$ were not critical in our experiments and did not affect PNPP conversion. Higher concentrations may produce problems, and steps to wash out or reduce the amount of serum through centrifugation are clearly required. The effect depends on the serum batch, and the serum should thus be checked for interference before routine use
	Inconsistent APH signal in cell/spheroid-containing wells	Incorrect pH of the assay buffer or the substrate solution, respectively	Check pH of the assay buffer as for the optimum detection of APH activity pH 4.8 ± 0.1 is required *Note*: we found a linear correlation between APH signal and cell counts per spheroid up to pH 7
	Incorrect APH assay signal	Inappropriate filter settings	Check filter settings of the microplate reader and lamp
10B (viii)	Critical variability or nonreproducibility of APH assay signal	High serum concentration in supernatant	See above
		Loss of cell material during transfer of spheroids, clusters and cells onto new uncoated 96-well plates	Carefully perform and monitor Steps 2–5 in the APH assay protocol for spheroids
		Highly variable spheroid size (and cell count per spheroid, respectively) before and/or after treatment	See above Always monitor spheroid integrity and size before and after treatment
		Inappropriate preparation of drug and treatment procedure	See above See Experimental design for additional discussion
14	Abnormal spheroid growth of controls	Contamination or incorrect incubation conditions	Check incubator and media

(continued)

TABLE 2 | Troubleshooting table (continued).

Step	Problem	Possible reason	Solution/action
		Inadequate medium refreshment	Exchange 50% of supernatant at least every other day following treatment Preheat medium before usage (according to routine cell culture instructions) and monitor pH
		Too few or too many passages of stock cultures or morphologically and/or genetically altered stock culture	Transfer cells at least twice after thawing and before spheroid initiation Limit usage of stock cultures to a defined narrow passage-window of >1 and <20 passages to sufficiently minimize the risk for accumulating new genetic alterations *Note*: some cell lines may even develop such alterations within a passage-window of <20 passages
		Monolayer cells used for initiation were not exponential	Define standard protocol according to instructions
15	Spheroid cell detachment	Disturbance of spheroids and cell shedding	Avoid medium exchange with high pressure and do not aspirate spheroids unless required for further analysis, e.g., spheroid dissociation
		Biological variability of tumor cells in spheroid culture in a pathophysiological 3D environment	Beware of the 'normal' disruption of large spheroids under stationary conditions, e.g., HT29, but not HCT-116, reach a spheroid volume plateau. HCT-116 spheroids consistently collapse within 48 h after reaching an average size of about 900–1,000 μm
		Drugs may affect cellular attachment but not viability and/or proliferative capacity	*Note*: this aspect is under investigation but is not routinely monitored as an analytical end point in our spheroid-based drug test system

ANTICIPATED RESULTS

Our protocol provides some routine, easy-handling and reliable tools that allow a direct and rapid comparison of drug efficacy in monolayer and spheroid culture. The initial analytical end point cell integrity as determined through the APH cell viability assay (**Fig. 5**) combined with the monitoring of spheroid integrity and volume growth (**Fig. 6**) is sufficient to identify drug candidates that lose efficacy in a 3D tissue structure and vice versa to approve those that target molecules or conditions developed in a 3D environment. The testing of numerous drugs that are in clinical use is envisioned to unequivocally prove the clinical predictive significance of the test strategy as compared with less complex assay systems and *in vivo* models. Spheroids can thus become a valid tool for negative and positive selection of the most promising candidates in drug development programs resulting in economical savings.

We identified the APH assay as a reliable and rapid handling tool for monitoring cell viability in single

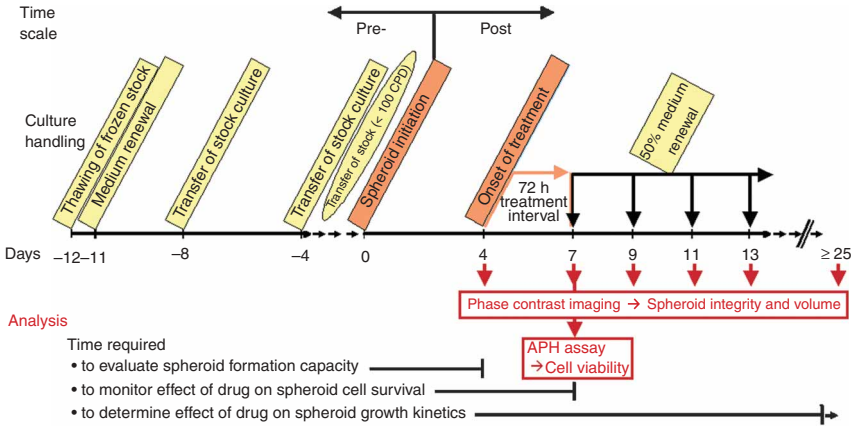

Figure 4 | Time table for setting up and performing standardized spheroid-based drug tests with established tumor cell lines using cell survival after treatment (APH assay) and growth delay (spheroid volume growth and regrowth, respectively) as analytical end points.

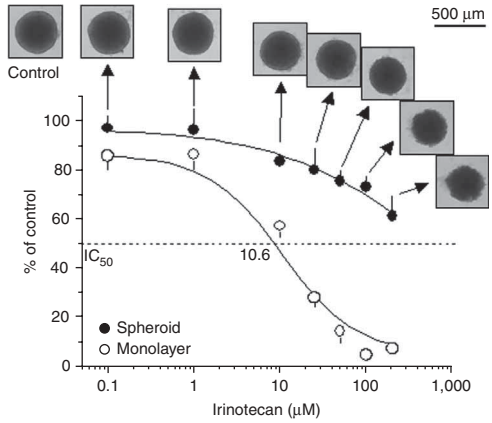

Figure 5 | Routine monitoring of drug effects on cell survival in HT29 colorectal cancer spheroids following drug treatment as determined through the acid phosphatase (APH) assay. Spheroid-based test protocol: liquid overlay in agarose-coated 96-well plates; seeding density 1.5×10^3 HT29 colon cancer cells per well in 200 µl of FCS-conditioned DMEM standard medium; initiation interval, 4 d; mean spheroid size at day 4 (onset of treatment), 370–400 µm; 72 h treatment interval. Graph shows relative cell viability in monolayer and spheroid cultures after 72 h of treatment with irinotecan. Data points are means ± standard deviation (s.d.) relative to untreated controls from one experiment with $n = 8$ individual spheroids per condition. IC_{50} values were calculated to emphasize the difference of drug efficacy in 2D versus 3D culture. Dose–response curves were recorded in three independent experimental series showing high reproducibility as shown in ref. 30. For the particular experiment presented herein, representative phase-contrast images are documented to capture spheroid integrity and volume following treatment at the time of cell survival assessment (magnification ×10 objective).

spheroids. In experiments throughout the past years, a total number of 8–16 spheroids per condition was found to be sufficient for evaluating cell survival after drug treatment and to calculate IC_{50} values from dose–response curves such as the one documented in **Figure 5** for the topoisomerase I inhibitor irinotecan (Toronto Research Chemicals TRC Inc.). The assay is simple and high-throughput compatible and shall be increasingly used to examine drug effects in spheroid cultures. In all cases, exponential monolayer cultures can serve as reference. The assay, however, is a one-state measurement and does not reflect clonogenic survival. Hence, combination with spheroid integrity and volume monitoring (**Fig. 6**), e.g., through phase-contrast imaging, is most useful. Data should be collected, and databases akin to the NCI-DTP 60 cell-line screen should become available to provide clear evidence that the spheroid model is able to aid in a better selection of clinically relevant drugs.

It is noted that the protocol allows significant basic screening but is not sufficient to identify the mechanisms leading to alterations in drug efficacy in 3D versus 2D culture. Limitations in drug penetration, contact-dependent multidrug resistence phenomena and oxygen deficiency are just three of the parameters influencing drug effects. Gene and protein expression modified by the 3D environment are further features that affect and potentially reflect treatment outcome. Indeed, in addition to the biochemical and histological advantages of tumor spheroids over traditional 2D culture as a cancer model, it is worth reiterating that there is increasing evidence that overall gene expression patterns in spheroids are more similar to those observed in real tumor samples[25,73–75]. Moreover, refined methods for monitoring a number of additional clinically relevant parameters have, in recent years, shown intriguing parallels between spheroid systems and authentic tumor samples. These include specific as well as overall gene expression differences in different tissue layers using reporter assays[76–78] as well as novel approaches to modeling drug distribution *in vivo*[71,79,80]. Furthermore, elegant studies to relate drug resistance phenomena in tumor tissue to these in cultured spheroids[18,34,81,82] have shown impressive similarities as well. Among other things, expression patterning may thus provide relevant mechanistic insight in the action of promising drug candidates, e.g., those identified through the basic screen.

Additional research is required to improve cell-line–based screens or extend our protocol to the use of primary tumor material. A particularly intriguing focus is the study of cell populations with cancer stem cell potential. Recent work indicates that tumor-initiating cell/cancer stem cell populations—to retain their stem cell characteristics in culture—may have to be

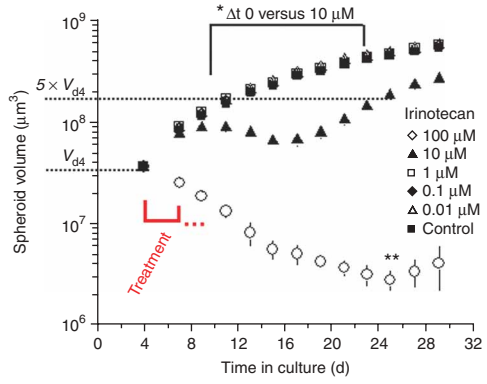

Figure 6 | Routine monitoring of spheroid growth/regrowth of drug-treated HT29 spheroids. Spheroid-based test protocol according to **Figure 5**; routine 72 h treatment interval without medium renewal followed by 50% medium exchange every 48 h for further culturing. Every feeding step results in a consecutive 1:2 dilution of the drug. Graph visualizes spheroid volume growth kinetics of HT29 spheroids in liquid overlay culture and evaluation of the parameter growth delay/regrowth as additional analytical end point of interest. Here growth delay is defined as the time lag of treated versus nontreated cultures to reach the quintuple spheroid volume of day 4 ($5 \times V_{d4}$; V_{d4} = spheroid volume at onset of treatment). Data points are mean spheroid volumes ± s.d. from $8 \leq n \leq 16$ spheroids. *HT29 spheroid growth delay treated with 10 µM irinotecan was about 14 d. **24 d after initial drug exposure spheroids treated with 100 µM irinotecan started to regrow.

propagated as spheroids (or spheres). Examples from the literature providing evidence for the existence of tumor-initiating cell/cancer stem cell populations in solid tumors include entities as diverse as glioblastomas, breast, renal, ovarian, pancreatic, gastric and colorectal cancers[83–88]. If the cancer stem cell hypothesis proves true, including the assumption that this subpopulation of cells shows higher treatment resistance or survival capacity in particular pathophysiological niches, this observation will have a clear and important impact on future experimental work, including the development of new, target-specific drugs.

ACKNOWLEDGMENTS We gratefully acknowledge the technical assistance of Marit Wondrak, Juana M Castaneda and Tammy Lawrence as well as Frank van Rey and Rupert Feldmeier. The experimental protocols and work documented herein were supported by the Society for Biomolecular Sciences (SBS) and by the German Federal Ministry of Education and Research (BMBF) through grants 0313143 and 01ZZ0502 to L.A.K.-S.

COMPETING INTERESTS STATEMENT The authors declare competing financial interests (see the HTML version of this article for details).

Published online at http://www.natureprotocols.com/
Reprints and permissions information is available online at http://npg.nature.com/reprintsandpermissions/

1. Abbott, A. Cell culture: biology's new dimension. *Nature* **424**, 870–872 (2003).
2. Kunz-Schughart, L.A., Freyer, J.P., Hofstaedter, F. & Ebner, R. The use of 3-D cultures for high-throughput screening: the multicellular spheroid model. *J. Biomol. Screen* **9**, 273–285 (2004).
3. Friedrich, J. *et al.* A reliable tool to determine cell viability in complex 3-d culture: the Acid phosphatase assay. *J. Biomol. Screen.* **12**, 925–937 (2007).
4. Gudjonsson, T., Ronnov-Jessen, L., Villadsen, R., Bissell, M.J. & Petersen, O.W. To create the correct microenvironment: three-dimensional heterotypic collagen assays for human breast epithelial morphogenesis and neoplasia. *Methods* **30**, 247–255 (2003).
5. Nelson, C.M. & Bissell, M.J. Modeling dynamic reciprocity: engineering three-dimensional culture models of breast architecture, function, and neoplastic transformation. *Semin. Cancer Biol.* **15**, 342–352 (2005).
6. Lee, G.Y., Kenny, P.A., Lee, E.H. & Bissell, M.J. Three-dimensional culture models of normal and malignant breast epithelial cells. *Nat. Methods* **4**, 359–365 (2007).
7. Friedrich, J., Ebner, R. & Kunz-Schughart, L.A. Experimental anti-tumor therapy in 3-D: spheroids—old hat or new challenge? *Int. J. Radiat. Biol.* **83**, 849–871 (2007).
8. Mueller-Klieser, W. Multicellular spheroids. A review on cellular aggregates in cancer research. *J. Cancer Res. Clin. Oncol.* **113**, 101–122 (1987).
9. Kunz-Schughart, L.A., Kreutz, M. & Knuechel, R. Multicellular spheroids: a three-dimensional *in vitro* culture system to study tumour biology. *Int. J. Exp. Pathol.* **79**, 1–23 (1998).
10. Santini, M.T. & Rainaldi, G. Three-dimensional spheroid model in tumor biology. *Pathobiology* **67**, 148–157 (1999).
11. Khaitan, D., Chandna, S., Arya, M.B. & Dwarakanath, B.S. Establishment and characterization of multicellular spheroids from a human glioma cell line: implications for tumor therapy. *J. Transl. Med.* **4**, 12 (2006).
12. Dubessy, C., Merlin, J.M., Marchal, C. & Guillemin, F. Spheroids in radiobiology and photodynamic therapy. *Crit. Rev. Oncol. Hematol.* **36**, 179–192 (2000).
13. Ballangrud, A.M. *et al.* Response of LNCaP spheroids after treatment with an alpha-particle emitter (213Bi)-labeled anti-prostate-specific membrane antigen antibody (J591). *Cancer Res.* **61**, 2008–2014 (2001).
14. Durand, R.E. & Olive, P.L. Resistance of tumor cells to chemo- and radiotherapy modulated by the three-dimensional architecture of solid tumors and spheroids. *Methods Cell Biol.* **64**, 211–233 (2001).
15. Mueller-Klieser, W. Three-dimensional cell cultures: from molecular mechanisms to clinical applications. *Am. J. Physiol.* **273**, C1109–C1123 (1997).
16. Al-Hajj, M., Becker, M.W., Wicha, M., Weissman, I. & Clarke, M.F. Therapeutic implications of cancer stem cells. *Curr. Opin. Genet. Dev.* **14**, 43–7 (2004).
17. Vermeulen, L. *et al.* Single-cell cloning of colon cancer stem cells reveals a multi-lineage differentiation capacity. *Proc. Natl. Acad. Sci. USA* **105**, 13427–13432 (2008).
18. Barbone, D., Yang, T.M., Morgan, J.R., Gaudino, G. & Broaddus, V.C. Mammalian target of rapamycin contributes to the acquired apoptotic resistance of human mesothelioma multicellular spheroids. *J. Biol. Chem.* **283**, 13021–13030 (2008).
19. Desoize, B. & Jardillier, J. Multicellular resistance: a paradigm for clinical resistance? *Crit. Rev. Oncol. Hematol.* **36**, 193–207 (2000).
20. Mueller-Klieser, W. Tumor biology and experimental therapeutics. *Crit. Rev. Oncol./Hematol.* **36**, 123–139 (2000).
21. Carlsson, J. & Acker, H. Relations between pH, oxygen partial pressure and growth in cultured cell spheroids. *Int. J. Cancer* **42**, 715–720 (1988).
22. Poland, J. *et al.* Comparison of protein expression profiles between monolayer and spheroid cell culture of HT-29 cells revealed fragmentation of CK18 in three-dimensional cell culture. *Electrophoresis* **23**, 1174–1184 (2002).
23. Frankel, A., Man, S., Elliott, P., Adams, J. & Kerbel, R.S. Lack of multicellular drug resistance observed in human ovarian and prostate carcinoma treated with the proteasome inhibitor PS-341. *Clin. Cancer Res.* **6**, 3719–3728 (2000).
24. Eshleman, J.S. *et al.* Inhibition of the mammalian target of rapamycin sensitizes U87 xenografts to fractionated radiation therapy. *Cancer Res.* **62**, 7291–7297 (2002).
25. Oloumi, A., Lam, W., Banath, J.P. & Olive, P.L. Identification of genes differentially expressed in V79 cells grown as multicell spheroids. *Int. J. Radiat. Biol.* **78**, 483–492 (2002).
26. Jelic, S. Molecular basis of future patients-tailored treatment. *Arch. Oncol.* **13**, 56–58 (2005).
27. Liu, M. *et al.* Antitumor activity of rapamycin in a transgenic mouse model of ErbB2-dependent human breast cancer. *Cancer Res.* **65**, 5325–5336 (2005).
28. Dardousis, K. *et al.* Identification of differentially expressed genes involved in the formation of multicellular tumor spheroids by HT-29 colon carcinoma cells. *Mol. Ther.* **15**, 94–102 (2007).
29. Howes, A.L. *et al.* The phosphatidylinositol 3-kinase inhibitor, PX-866, is a potent inhibitor of cancer cell motility and growth in three-dimensional cultures. *Mol. Cancer Ther.* **6**, 2505–2514 (2007).
30. Kunz-Schughart, L.A. Multicellular tumor spheroids: intermediates between monolayer culture and *in vivo* tumor. *Cell Biol. Int.* **23**, 157–161 (1999).
31. Furbert-Harris, P.M. *et al.* Eosinophils in a tri-cell multicellular tumor spheroid (MTS)/endothelium complex. *Cell Mol. Biol.* **49**, 1081–1088 (2003).
32. Gottfried, E., Kunz-Schughart, L.A., Andreesen, R. & Kreutz, M. Brave little world: spheroids as an *in vitro* model to study tumor-immune-cell interactions. *Cell Cycle* **5**, 691–695 (2006).
33. Spoettl, T. *et al.* Monocyte chemoattractant protein-1 (MCP-1) inhibits the intestinal-like differentiation of monocytes. *Clin. Exp. Immunol.* **145**, 190–199 (2006).
34. Wartenberg, M., Finkensieper, A., Hescheler, J. & Sauer, H. Confrontation cultures of embryonic stem cells with multicellular tumor spheroids to study tumor-induced angiogenesis. *Methods Mol. Biol.* **331**, 313–328 (2006).
35. Gunther, S. *et al.* Polyphenols prevent cell shedding from mouse mammary cancer spheroids and inhibit cancer cell invasion in confrontation cultures derived from embryonic stem cells. *Cancer Lett.* **250**, 25–35 (2007).
36. Li, Z.W. & Dalton, W.S. Tumor microenvironment and drug resistance in hematologic malignancies. *Blood Rev.* **20**, 333–342 (2006).
37. Kunz-Schughart, L.A. & Mueller-Klieser, W. Three-dimensional culture. In *Animal Cell Culture* Vol. 3 (Ed. Masters, J.R.W.) 123–148 (Oxford University Press, Oxford, 2000).
38. Stark, H.J., Baur, M., Breitkreutz, D., Mirancea, N. & Fusenig, N.E. Organotypic keratinocyte cocultures in defined medium with regular epidermal morphogenesis and differentiation. *J. Invest. Dermatol.* **112**, 681–691 (1999).
39. Stark, H.J. *et al.* Epidermal homeostasis in long-term scaffold-enforced skin equivalents. *J. Investig. Dermatol. Symp. Proc.* **11**, 93–105 (2006).
40. Korff, T. & Augustin, H.G. Integration of endothelial cells in multicellular spheroids prevents apoptosis and induces differentiation. *J. Cell Biol.* **143**, 1341–1352 (1998).
41. Ivascu, A. & Kubbies, M. Rapid generation of single-tumor spheroids for high-throughput cell function and toxicity analysis. *J. Biomol. Screen* **11**, 922–932 (2006).
42. Kosaka, T. *et al.* Comparison of various methods of assaying the cytotoxic effects of ethanol on human hepatoblastoma cells (HUH-6 line). *Acta. Med. Okayama* **50**, 151–156 (1996).
43. Enmon, R. *et al.* Combination treatment with 17-*N*-allylamino-17-demethoxy geldanamycin and acute irradiation produces supra-additive growth suppression in human prostate carcinoma spheroids. *Cancer Res.* **63**, 8393–8399 (2003).

44. Fehlauer, F. *et al.* Effects of irradiation and cisplatin on human glioma spheroids: inhibition of cell proliferation and cell migration. *J. Cancer Res. Clin. Oncol.* **131**, 723–732 (2005).
45. Lambert, B. *et al.* Screening for supra-additive effects of cytotoxic drugs and gamma irradiation in an *in vitro* model for hepatocellular carcinoma. *Can. J. Physiol. Pharmacol.* **82**, 146–152 (2004).
46. Sutherland, R.M. Cell and environment interactions in tumor microregions: the multicell spheroid model. *Science* **240**, 177–184 (1988).
47. LaRue, K.E., Khalil, M. & Freyer, J.P. Microenvironmental regulation of proliferation in multicellular spheroids is mediated through differential expression of cyclin-dependent kinase inhibitors. *Cancer Res.* **64**, 1621–1631 (2004).
48. Francia, G., Man, S., Teicher, B., Grasso, L. & Kerbel, R.S. Gene expression analysis of tumor spheroids reveals a role for suppressed DNA mismatch repair in multicellular resistance to alkylating agents. *Mol. Cell. Biol.* **24**, 6837–6849 (2004).
49. Francia, G. *et al.* Down-regulation of DNA mismatch repair proteins in human and murine tumor spheroids: implications for multicellular resistance to alkylating agents. *Mol. Cancer Ther.* **4**, 1484–1494 (2005).
50. Bindra, R.S., Crosby, M.E. & Glazer, P.M. Regulation of DNA repair in hypoxic cancer cells. *Cancer Metastasis Rev* **26**, 249–260 (2007).
51. Romero, F.J., Zukowski, D. & Mueller-Klieser, W. Glutathione content of V79 cells in two- or three-dimensional culture. *Am. J. Physiol.* **272**, C1507–C1512 (1997).
52. Winters, B.S., Raj, B.K., Robinson, E.E., Foty, R.A. & Corbett, S.A. Three-dimensional culture regulates Raf-1 expression to modulate fibronectin matrix assembly. *Mol. Biol. Cell* **17**, 3386–3396 (2006).
53. Carlsson, J. & Yuhas, J.M. Liquid-overlay culture of cellular spheroids. *Recent Results Cancer Res.* **95**, 1–23 (1984).
54. Tong, J.Z. *et al.* Long-term culture of adult rat hepatocyte spheroids. *Exp. Cell Res.* **200**, 326–332 (1992).
55. Hoevel, T., Macek, R., Swisshelm, K. & Kubbies, M. Reexpression of the TJ protein CLDN1 induces apoptosis in breast tumor spheroids. *Int. J. Cancer* **108**, 374–383 (2004).
56. Wartenberg, M. *et al.* Development of an intrinsic P-glycoprotein-mediated doxorubicin resistance in quiescent cell layers of large, multicellular prostate tumor spheroids. *Int. J. Cancer* **75**, 855–863 (1998).
57. Kunz-Schughart, L.A. & Freyer, J.P. Adaptation of an automated selective dissociation procedure to two novel spheroid types. *In Vitro Cell. Dev. Biol. Anim.* **33**, 73–76 (1997).
58. Kerr, D.J., Wheldon, T.E., Kerr, A.M. & Kaye, S.B. *In vitro* chemosensitivity testing using the multicellular tumor spheroid model. *Cancer Drug Deliv.* **4**, 63–74 (1987).
59. Durand, R.E. Slow penetration of anthracyclines into spheroids and tumors: a therapeutic advantage? *Cancer Chemother. Pharmacol.* **26**, 198–204 (1990).
60. Freyer, J.P. & Schor, P.L. Automated selective dissociation of cells from different regions of multicellular spheroids. *In Vitro Cell Dev. Biol.* **25**, 9–19 (1989).
61. Watanabe, N., Hirayama, R. & Kubota, N. The chemopreventive flavonoid apigenin confers radiosensitizing effect in human tumor cells grown as monolayers and spheroids. *J. Radiat. Res. (Tokyo)* **48**, 45–50 (2007).
62. Essand, M., Nilsson, S. & Carlsson, J. Growth of prostatic cancer cells, DU 145, as multicellular spheroids and effects of estramustine. *Anticancer Res.* **13**, 1261–1268 (1993).
63. Russell, J., Wheldon, T.E. & Stanton, P. A radioresistant variant derived from a human neuroblastoma cell line is less prone to radiation-induced apoptosis. *Cancer Res.* **55**, 4915–4921 (1995).
64. Marusic, M., Bajzer, Z., Vuk-Pavlovic, S. & Freyer, J.P. Tumor growth *in vivo* and as multicellular spheroids compared by mathematical models. *Bull. Math. Biol.* **56**, 617–631 (1994).
65. Kunz-Schughart, L.A., Groebe, K. & Mueller-Klieser, W. Three-dimensional cell culture induces novel proliferative and metabolic alterations associated with oncogenic transformation. *Int. J. Cancer* **66**, 578–586 (1996).
66. Tabatabai, M., Williams, D.K. & Bursac, Z. Hyperbolastic growth models: theory and application. *Theor. Biol. Med. Model.* **2**, 14–15 (2005).
67. Mellor, H.R., Ferguson, D.J. & Callaghan, R. A model of quiescent tumour microregions for evaluating multicellular resistance to chemotherapeutic drugs. *Br. J. Cancer* **93**, 302–309 (2005).
68. Orlandi, P. *et al.* Idarubicin and idarubicinol effects on breast cancer multicellular spheroids. *J. Chemother.* **17**, 663–667 (2005).
69. Lambert, B. *et al.* Assessment of supra-additive effects of cytotoxic drugs and low dose rate irradiation in an *in vitro* model for hepatocellular carcinoma. *Can. J. Physiol. Pharmacol.* **84**, 1021–1028 (2006).
70. Hirschberg, H., Sun, C.H., Krasieva, T. & Madsen, S.J. Effects of ALA-mediated photodynamic therapy on the invasiveness of human glioma cells. *Lasers Surg. Med.* **38**, 939–945 (2006).
71. Minchinton, A.I. & Tannock, I.F. Drug penetration in solid tumours. *Nat. Rev. Cancer* **6**, 583–592 (2006).
72. Xiao, Z., Hansen, C.B., Allen, T.M., Miller, G.G. & Moore, R.B. Distribution of photosensitizers in bladder cancer spheroids: implications for intravesical instillation of photosensitizers for photodynamic therapy of bladder cancer. *J. Pharm. Pharm. Sci.* **8**, 536–543 (2005).
73. L'Esperance, S., Bachvarova, M., Tetu, B., Mes-Masson, A.M. & Bachvarov, D. Global gene expression analysis of early response to chemotherapy treatment in ovarian cancer spheroids. *BMC Genomics* **9**, 99 (2008).
74. Shiras, A., Bhosale, A., Patekar, A., Shepal, V. & Shastry, P. Differential expression of CD44(S) and variant isoforms v3, v10 in three-dimensional cultures of mouse melanoma cell lines. *Clin. Exp. Metastasis* **19**, 445–455 (2002).
75. Zietarska, M. *et al.* Molecular description of a 3D *in vitro* model for the study of epithelial ovarian cancer (EOC). *Mol. Carcinog.* **46**, 872–885 (2007).
76. Berchner-Pfannschmidt, U. *et al.* Nuclear oxygen sensing: induction of endogenous prolyl-hydroxylase 2 activity by hypoxia and nitric oxide. *J. Biol. Chem.* **83**, 31745–31753 (2008).
77. Leroux, F. *et al.* Experimental approaches to kinetics of gas diffusion in hydrogenase. *Proc. Natl. Acad. Sci. USA* **105**, 11188–11193 (2008).
78. Nowicki, M.O. *et al.* Lithium inhibits invasion of glioma cells; possible involvement of glycogen synthase kinase-3. *Neuro Oncol.* **10**, 690–699 (2008).
79. Wartenberg, M., Hescheler, J. & Sauer, H. Electrical fields enhance growth of cancer spheroids by reactive oxygen species and intracellular Ca2+. *Am. J. Physiol.* **272**, R1677–R1683 (1997).
80. Gali-Muhtasib, H. *et al.* Thymoquinone triggers inactivation of the stress response pathway sensor CHEK1 and contributes to apoptosis in colorectal cancer cells. *Cancer Res.* **68**, 5609–5618 (2008).
81. Wartenberg, M. *et al.* Reactive oxygen species-linked regulation of the multidrug resistance transporter P-glycoprotein in Nox-1 overexpressing prostate tumor spheroids. *FEBS Lett.* **579**, 4541–4549 (2005).
82. Salmaggi, A. *et al.* Glioblastoma-derived tumorospheres identify a population of tumor stem-like cells with angiogenic potential and enhanced multidrug resistance phenotype. *Glia* **54**, 850–860 (2006).
83. Singh, S.K. *et al.* Identification of human brain tumour initiating cells. *Nature* **432**, 396–401 (2004).
84. Hermann, P.C. *et al.* Distinct populations of cancer stem cells determine tumor growth and metastatic activity in human pancreatic cancer. *Cell Stem Cell* **1**, 313–323 (2007).
85. O'Brien, C.A., Pollett, A., Gallinger, S. & Dick, J.E. A human colon cancer cell capable of initiating tumour growth in immunodeficient mice. *Nature* **445**, 106–110 (2007).
86. Ricci-Vitiani, L. *et al.* Identification and expansion of human colon-cancer-initiating cells. *Nature* **445**, 111–115 (2007).
87. Mizrak, D., Brittan, M. & Alison, M.R. CD133: molecule of the moment. *J. Pathol.* **214**, 3–9 (2008).
88. Takaishi, S., Okumura, T. & Wang, T.C. Gastric cancer stem cells. *J. Clin. Oncol.* **26**, 2876–2882 (2008).
89. Chen, T.R., Dorotinsky, C.S., McGuire, L.J., Macy, M.L. & Hay, R.J. DLD-1 and HCT-15 cell lines derived separately from colorectal carcinomas have totally different chromosome changes but the same genetic origin. *Cancer Genet. Cytogenet.* **81**, 103–108 (1995).
90. Roschke, A.V. *et al.* Karyotypic 'state' as a potential determinant for anticancer drug discovery. *Proc. Natl. Acad. Sci. USA* **102**, 2964–2969 (2005).
91. Ellison, G. *et al.* Further evidence to support the melanocytic origin of MDA-MB-435. *Mol. Pathol.* **55**, 294–299 (2002).
92. Rae, J.M. *et al.* Common origins of MDA-MB-435 cells from various sources with those shown to have melanoma properties. *Clin. Exp. Metastasis* **21**, 543–552 (2004).
93. Garraway, L.A. *et al.* Integrative genomic analyses identify MITF as a lineage survival oncogene amplified in malignant melanoma. *Nature* **436**, 117–122 (2005).